# Theoretical Basis for Experimental Design of Radial Diffusion Tests

M. Takeda, M. Zhang, H. Nakajima, T. Hiratsuka
National Institute of Advanced Industrial Science and Technology (AIST)
Research Center for Deep Geological Environments
Higashi 1-1-1, Central 7, Tsukuba, Ibaraki 305-8567
Japan

## ABSTRACT

Evaluation of the directional diffusivities and adsorptive properties of natural barrier materials is of fundamental importance in the design and assessment of the geological disposal of hazardous contaminants including radioactive nuclear wastes.

In order to facilitate evaluation of the directional diffusivities of anisotropic media, a single-reservoir radial diffusion test for cylindrical specimens is proposed and an analytical solution corresponding to the experimental configuration of the proposed test is derived in this study. The feasibility of the diffusion test depends on whether the experiment can be performed within a reasonable period and whether reliable parameter estimation is ensured. In order to examine these factors for the proposed test, a feasibility study based on theoretical and numerical examinations was performed.

A series of examinations showed that the use of a sorptive tracer is advantageous for both obtaining measurement data within a short period of time and for increasing parameter sensitivity; however these also depend on selected experimental conditions, such as the dimensions of the specimen and the reservoir. The effects of the tracer properties and the other experimental conditions can be represented by the dimensionless reservoir volume defined as the ratio of reservoir volume over the adsorptive capacity of the specimen. Therefore, in designing experiments, it is important to evaluate the value of the dimensionless reservoir volume based on the information available for the testing material and the tracer.

When the effective diffusion coefficient of the testing material is very small, the duration of the experiment becomes very long. In such a case, a practical way of determining the values of the parameters is inverse analysis of the transient data. In order to clarify the applicability and limitations of inverse analysis for the proposed test, typical inverse methods are briefly summarized and some considerations are made, especially as regards characterization and conditioning of the weighted Jacobian matrix for the inverse analyses. Characterization of the weighted Jacobian matrix for the proposed test revealed that the weighted Jacobian matrix is not necessarily well-conditioned, owing to differences in the orders of magnitude between the values of the effective diffusion coefficient and the capacity factor. A promising way of conditioning the weighted Jacobian matrix is also introduced.

## INTRODUCTION

Safety assessments of facilities involved in geological disposal of hazardous wastes, including radioactive nuclear waste, are generally performed through mass transport simulations. Transport of contaminants, such as radionuclides, through an engineered and natural barrier system is mainly controlled by advection, dispersion, sorption and chain decay. When groundwater flow is very slow, the most important mechanisms of transport and retardation are diffusion through and sorption onto the barrier materials, and thus evaluation of relevant parameters, particularly the effective diffusion coefficient and capacity factor, is of fundamental importance in safety assessments [e.g., 1-10].

The diffusion of substances in porous media is known to depend on the geometric orientation of the pore structure [e.g., 10,11]. For example, preferentially layered pore structures due to sedimentation in sedimentary rocks may cause anisotropic diffusion in directions perpendicular and parallel to the bedding plane. Thus, in order to evaluate diffusion phenomena in anisotropic media, directional diffusivities should be investigated, especially when the pore structure in a medium cannot be ideally considered to be isotropic.

For measurement of diffusive and adsorptive properties, such as the effective diffusion coefficient and the capacity factor, many types of laboratory diffusion tests have been developed. Most tests, however, are designed for determining diffusivity in the axial direction of cylindrical specimens cored from boreholes or molded in a laboratory [12-14]. Thus, in order to derive a full understanding of the directional diffusivities of anisotropic media, combination of the diffusion tests evaluating diffusivities in the different directions is needed.

To evaluate the directional diffusivity as a 2D tensor, several radial diffusion tests for hollow cylindrical specimens have been developed [11,15,16]. However, these tests require relatively tedious experimental procedures, such as the intermittent replacement of reservoir solutions until steady state data is obtained and/or specimen preparation in which a cylindrical specimen is shaped into a hollow cylinder.

In order to facilitate estimation of the radial diffusivity of a cylindrical specimen, a single-reservoir radial diffusion test for a cylindrical specimen is proposed in this study. The advantage of this test over those for a hollow cylindrical specimen is the simple experimental configuration. Furthermore, the proposed test would facilitate double testing of a cylindrical specimen, by both radial and 1D diffusion tests, which would provide better understanding of the directional diffusivity of materials with geometric orientations of pore structures, especially preferentially layered sediments.

As will be shown in the following section, the analytical solution for the single-reservoir radial diffusion test for a cylindrical specimen introduced in this study is nonlinear with respect to the effective diffusion coefficient and capacity factor during the transient state, as for a hollow cylindrical specimen. Thus, inverse analyses for the parameter estimation are indispensable for the radial-diffusion tests, especially when the diffusivities of the testing materials are very low, so the steady or equilibrium states are not established within reasonable experimental periods.

In order to examine the applicability of the inverse analysis to the radial-diffusion tests, the typical inverse analysis methods are briefly summarized, and potential problems related to parameter estimation based on transient data analysis are discussed, using the proposed radial-diffusion test as an example.

Finally, the feasibility of the proposed test method is examined through a series of numerical simulations in which the dependencies of the experimental duration and the sensitivities of the measurement data on the experimental conditions are evaluated.

## SINGLE-RESERVOIR RADIAL DIFFUSION TEST

### Experimental configuration

In Fig. 1, the single-reservoir radial diffusion test for a cylindrical specimen (being proposed in this study) is compared to radial diffusion tests that use a hollow cylindrical specimen. In the constant inner concentration with constant outer concentration test for the hollow specimen (Fig. 1 (a)), the transient variation of the diffused flux is measured at the outer reservoir and the steady state flux is analyzed [11,15]. Control of the concentrations and measurement of the flux are usually accomplished by intermittent replacement of reservoir solutions and measurement of the concentration of the replaced solutions. Thus, laborious procedures are required until the steady state is established. In the single-reservoir radial diffusion test for a hollow specimen (Fig. 1 (b)), a known amount of tracer is injected into the source reservoir located inside the specimen and the transient variation in the solute concentration in

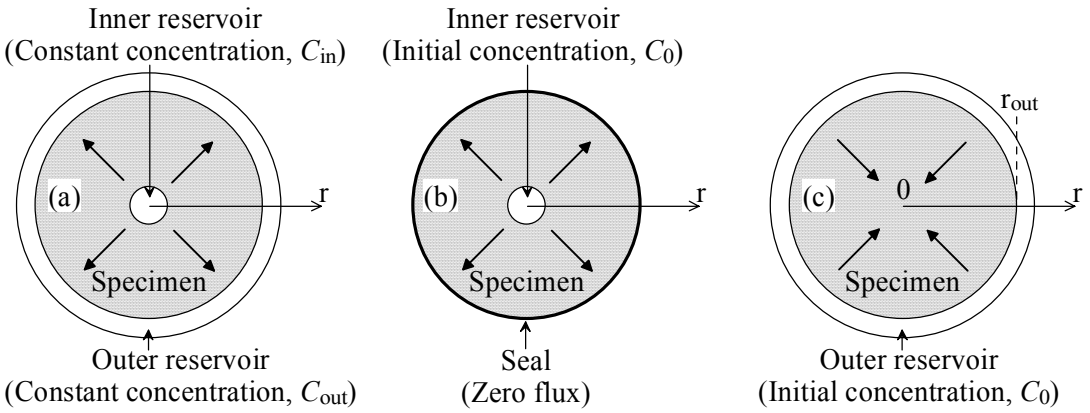


Fig. 1. Schematics of radial diffusion tests. (a)Constant inner concentration with constant outer concentration radial diffusion test for a hollow cylindrical specimen. (b)Single-reservoir radial diffusion test for a hollow cylindrical specimen. (c)Single-reservoir radial diffusion test for a cylindrical specimen. Arrows with bold lines indicate diffusion direction in the specimens.

the inner reservoir is measured. For the parameter estimation, the transient data are analyzed by inverse analysis [16]. In the single-reservoir radial diffusion test for a cylindrical specimen (Fig. 1 (c)), the tracer is injected into the outer reservoir and the transient variation of the solute concentration in the outer reservoir is measured and analyzed. The difference between the single-reservoir radial diffusion tests is the location of the source reservoir (Fig. 1 (b) and(c)). In contrast to the other two methods, the single-reservoir radial diffusion test for a cylindrical specimen does not require shaping of the cylindrical specimen into a hollow cylinder. The only requirements are sealing the top and bottom ends of the specimen and settling the prepared specimen in the solution reservoir. In the other methods for a hollow cylindrical specimen, sealing the exterior of the specimen or setting the inner solution reservoir is also required.

## Mathematical formulation and analytical solution

Assuming a linear sorption model, the radial diffusion of a solute in a porous medium under transient conditions can be described by Fick's second law:

$$\frac{\partial^2 C}{\partial r^2}+\frac{1}{r}\cdot\frac{\partial C}{\partial r}-\frac{\alpha}{D_e}\cdot\frac{\partial C}{\partial t}=0\,, \qquad \text{(Eq. 1)}$$

where $C$ is the solute concentration [$ML^{-3}$] in porewater; $t$ and $r$ are the time [T] and distance [L], and $D_e$ and $\alpha$ are the effective diffusion coefficient in the radial direction [$L^2T^{-1}$] and the capacity factor of the porous medium [-], respectively.

Assuming that the specimen has a radius, $r_{out}$ [L], and that the center and exterior of the specimen are located at $r$=0 and $r$=$r_{out}$, respectively, on radial coordinates, the initial condition is expressed as:

$$C(r,0)=0 \qquad 0\le r<r_{out}\,. \qquad \text{(Eq. 2)}$$

At the center of the specimen, zero flux can be assumed as:

$$\frac{\partial C}{\partial r}=0 \qquad t>0,\quad r=0\,. \qquad \text{(Eq. 3)}$$

The tracer injection and the reservoir concentration variation are expressed as:

$$C(r_{out},0)=C_0\,, \qquad \text{(Eq. 4)}$$

$$\frac{\partial C}{\partial r}+\frac{V_r}{2\cdot\pi\cdot r_{out}\cdot D_e\cdot L}\cdot\frac{\partial C}{\partial t}=0 \qquad t>0,\quad r=r_{out}\,, \qquad \text{(Eq. 5)}$$

where $C_0$ is the initial solute concentration [$ML^{-3}$] in the source reservoir and $V_r$ is the reservoir volume [$L^3$]. Although $V_r$ represents the solution volumes in the source reservoir, it is referred to as the reservoir volume hereafter.

In order to facilitate comparisons between different experimental conditions, normalization of the analytical model is carried out by introducing the following dimensionless parameters into Eqs. 1 through 5:

$$c = \frac{C}{C_0}, \qquad \text{(Eq. 6)}$$

$$\tau = \frac{D_e \cdot t}{\alpha \cdot r_{out}^2}, \qquad \text{(Eq. 7)}$$

$$\rho = \frac{r}{r_{out}}, \qquad \text{(Eq. 8)}$$

$$\beta_r = \frac{V_r}{2 \cdot \pi \cdot r_{out}^2 \cdot L \cdot \alpha}, \qquad \text{(Eq. 9)}$$

where $c$ is the dimensionless solute concentration, $\rho$ the dimensionless distance, $\tau$ the dimensionless time, and $\beta_r$ the dimensionless reservoir volume defined as the ratio of the reservoir volume over the adsorptive capacity of the specimen. Using the above dimensionless parameters, Eqs. (1) through (5) are expressed as the following normalized forms:

$$\frac{\partial^2 c}{\partial \rho^2} + \frac{1}{\rho} \cdot \frac{\partial c}{\partial \rho} - \frac{\partial c}{\partial \tau} = 0, \qquad \text{(Eq. 1')}$$

$$c(\rho,0) = 0 \qquad 0 \le \rho < 1, \qquad \text{(Eq. 2')}$$

$$\frac{\partial c}{\partial \rho} = 0 \qquad \tau > 0, \quad \rho = 0, \qquad \text{(Eq. 3')}$$

$$c(1,0) = 1, \qquad \text{(Eq. 4')}$$

$$\frac{\partial c}{\partial \rho} + \beta_r \cdot \frac{\partial c}{\partial \tau} = 0 \qquad \tau > 0, \quad \rho = 1. \qquad \text{(Eq. 5')}$$

By the above treatment, dimensioned parameters are lumped into relevant dimensionless parameters and the number of parameters necessary for describing the single-reservoir radial diffusion test for a cylindrical specimen is reduced to a minimum.

By solving the normalized governing equation together with the normalized initial and boundary conditions, an analytical solution can be derived as:

$$c(\rho,\tau) = \frac{2 \cdot \beta_r}{2 \cdot \beta_r + 1} + \sum_{n=1}^{\infty} \frac{2 \cdot \exp\left(-\phi_n^2 \cdot \tau\right) \cdot \beta_r \cdot \phi_n \cdot J_0(\phi_n \cdot \rho)}{(\beta_r + 1) \cdot \phi_n \cdot J_0(\phi_n) - \left(\beta_r \cdot \phi_n^2 + 1\right) \cdot J_1(\phi_n)}, \qquad \text{(Eq. 10)}$$

where $J_0$ and $J_1$ are Bessel functions of the first kind, and $\varphi_n$ are the positive roots of:

$$\beta_r \cdot \phi = -\frac{J_1(\phi)}{J_0(\phi)}. \qquad \text{(Eq. 11)}$$

As described above, transient variations of the solute concentration in the single-reservoir radial diffusion test for the cylindrical specimen (Fig. 1 (c)) are expressed by multiplying the dimensionless solute concentration, $c(\rho,\tau)$, by the initial concentration in the source reservoir of $C_0$.

The initial concentration in the reservoir, $C_0$, is irrelevant to the transient variations of solute concentration in both the dimensionless and the dimensioned time scales. In the dimensionless forms, the dimensionless time, $\tau$, represents the actual time, $t$, and the specimen properties and dimensions (Eq. 7). In other words, the experimental time, $t$, for a certain specimen is represented by the dimensionless time, $\tau$, independent of the other condition, i.e., the reservoir volume, $V_r$. On the other hand, the dimensionless

reservoir volume, $\beta_r$, indicates the experimental condition, i.e., the reservoir volume, as well as the specimen properties and dimensions (Eq. 9). Accordingly, comparing the experimental durations in the dimensionless time scale between the different values of $\beta_r$ is equivalent to comparing the experimental durations in the actual time scale between different experimental conditions, assuming a specimen with certain dimensions and properties.

### Test interpretation

As shown by Eq. 10, the transient variations of solute concentrations are nonlinear with respect to the effective diffusion coefficient and the capacity factor; however the solute concentrations between the reservoir and pore spaces in the specimen are balanced at the equilibrium state. When time elapses, the equilibrium state is established. The equilibrium concentration can be calculated by setting $\tau \rightarrow \infty$ in Eq. 10:

$$c_{eq} = \frac{2 \cdot \beta_r}{2 \cdot \beta_r + 1}, \qquad \text{(Eq. 12)}$$

where $c_{eq}$ is the equilibrium concentration normalized with the initial concentration, $C_0$. Using Eq. 12 and the equilibrium concentration, the capacity factor, $\alpha$, can be estimated. Otherwise, the distribution coefficient, $K_d$, is estimated based on the mass balance consideration as in the batch sorption experiment [17]. The value of $K_d$ is estimated by the following expression:

$$K_d = \frac{C_0 - C_{eq}}{C_{eq}} \cdot \frac{\varepsilon}{\rho_b}, \qquad \text{(Eq. 13)}$$

where $\varepsilon$ and $\rho_b$ are the porosity and bulk density of the specimen.

As described above, the adsorptive property of the testing material might be estimated from the equilibrium concentration; however the experimental time would be significantly long when the testing material has a small diffusivity, as shown by Eq. 7. For that case, transient data analysis is useful because it might enable estimating both the diffusive and adsorptive values from the transient data. However, inverse analysis is required owing to the nonlinearity of the analytical solution with respect to the parameters of interest (Eq. 10).

## INVERSE ANALYSIS

In this paper, the feasibility of inverse analysis for the radial diffusion tests is a main concern, and problems related to this are illustrated by using the single-reservoir radial diffusion test for a cylindrical specimen as an example.

As described, an analytical solution to the single-reservoir radial diffusion test for a cylindrical specimen is nonlinear with respect to the parameters of interest during the transient phase. Even if the capacity factor can be estimated from the equilibrium concentration, the effective diffusion has to be inversely determined from the transient data. Accordingly, the parameter estimation should be performed with the inverse analysis by matching the functional model, i.e., the analytical solution, Eq. 10, with the observations, i.e., the transient variations of reservoir concentrations.

However, in inverse analyses, it is often difficult to derive a unique result depending on the characteristics of the objective function or the inverse problem itself, and the quality of the parameter estimation is affected by the sensitivities of the measurement data as well as the other factors, such as the measurement and systematic errors, and computational methods used in the inverse analyses. Therefore, examining these problems with respect to the radial diffusion tests is indispensable for examining the feasibilities of the radial diffusion tests.

In order to clarify the subjects to be discussed in the following sections, some basic concepts of inverse analysis are presented here, with emphasis on the aspects relevant to this study.

## Objective function

In inverse analyses, an objective function measuring the overall difference between observed data and the corresponding simulation results is minimized by adjusting parameters involved in the functional model (analytical solution in this study). According to Finstrele and Njita [18], the objective function is generally defined in the following form:

$$S = \sum_{i=1}^{m} \omega(y_i; \mathbf{p}), \qquad \text{(Eq. 14)}$$

where ω is a loss function and $y_i$ is a function of the weighted residual:

$$y_i = \frac{z_i^* - z_i(\mathbf{p})}{\sigma_{z_i}}, \qquad \text{(Eq. 15)}$$

where $z_i^*$ is one of m actual data points at a discrete point i in time and/or space, and $z_i$ is the corresponding variable calculated from the functional model. The parameter vector **p** of length n (<m) is a set of parameters to be estimated. The weighting coefficient $\sigma_{zi}$ is the standard deviation of the measurement error.

Separately from the direct minimization of Eq. 14, assuming that the measurement errors are normally distributed with mean zero and covariance matrix $\mathbf{C}_{zz}$ and follow the maximum likelihood theory, the degree of likelihood that the parameter set, **p,** produces the measurement data, $\mathbf{z}^*$, is expressed as:

$$L(\mathbf{p}; \mathbf{z}^*) = (2 \cdot \pi)^{-\frac{m}{2}} \cdot |\mathbf{C}_{zz}|^{-\frac{1}{2}} \cdot \exp\left[ -\frac{1}{2} \cdot (\mathbf{z}^* - \mathbf{z}(\mathbf{p}))^T \mathbf{C}_{zz}^{-1} (\mathbf{z}^* - \mathbf{z}(\mathbf{p})) \right]. \qquad \text{(Eq. 16)}$$

In order to estimate the parameter set, **p**, maximizing Eq. 16, the following negative log-likelihood or support criterion is used in the maximum likelihood estimation:

$$\begin{aligned} \Gamma &= -2 \cdot \ln\left[ L(\mathbf{p}; \mathbf{z}^*) \right] \\ &= m \cdot \ln(2 \cdot \pi) + \ln|\mathbf{C}_{zz}| + \left[ (\mathbf{z}^* - \mathbf{z}(\mathbf{p}))^T \mathbf{C}_{zz}^{-1} (\mathbf{z}^* - \mathbf{z}(\mathbf{p})) \right]. \end{aligned} \qquad \text{(Eq. 17)}$$

The minimization of Eq. 17 is equivalent to minimizing the sum of squares of weighted residuals:

$$X^2 = (\mathbf{z}^* - \mathbf{z}(\mathbf{p}))^T \mathbf{C}_{zz}^{-1} (\mathbf{z}^* - \mathbf{z}(\mathbf{p})). \qquad \text{(Eq. 18)}$$

Eq. 18 is the objective function for the maximum likelihood estimation. Moreover, assuming a lack of correlation among measurement errors, the error covariance matrix reduces to a diagonal matrix that can be written as $\mathbf{C}_{zz}=\sigma_0^2 \cdot \mathbf{V}_{zz}$. For this case, the maximum likelihood estimation using Eq. 18 is equivalent to the weighted least square estimation directly minimizing the objective function, Eq. 14. $\mathbf{V}_{zz}$ is a positive definite diagonal matrix which contains information on the error structure of the measurements. Although $\sigma_0^2$ can assume any positive value, it is convenient to set it to one and work with the actual covariance matrix $\mathbf{C}_{zz}$ rather than $\mathbf{V}_{zz}$.

When different types of error distributions are assumed, different loss functions and estimators are selected as summarized by Finstrele and Njita [18] or Carrera et al. [19]. When prior information on the parameters of interest is available, the separately estimated values for the parameters can be included in the observed data, i.e., $\mathbf{z}^*$, to regularize the problem and constrain the estimation [20].

## Minimization algorithm

In inverse analyses associated with model identification and parameter estimation in the field of subsurface hydrology, gradient-based iterative algorithms have frequently been adopted for minimizing the objective functions (e.g., 17-22). Among the gradient-based methods, Newton-type minimization algorithms with quadratic approximation of the objective function, i.e., Gauss-Newton or Levenberg-Marquardt algorithms, are preferred. In Newton's method, the objective function is locally approximated by a quadratic form which allows iterative computation of an improved parameter vector $\mathbf{p}_{k+1}$ from a previous estimation $\mathbf{p}_k$ as follows:

$$\mathbf{p}_{k+1} = \mathbf{p}_k - \mathbf{H}_k^{-1} \cdot \mathbf{g}_k , \quad \text{(Eq. 19)}$$

where k indicates the iterative step; $\mathbf{H}_k$ and $\mathbf{g}_k$ are the Hessian matrix with n×n components and gradient vector of the objective function in n-dimensional parameter space, respectively.

For the objective function defined as the sum of squares of weighted residuals, Eq. 19 can be expressed as:

$$\mathbf{p}_{k+1} = \mathbf{p}_k - \frac{1}{2} \cdot \left[ \mathbf{J}_k^T \cdot \mathbf{J}_k + \sum_{i=1}^{m} y_i \cdot \mathbf{G}_k \right]^{-1} \cdot \mathbf{g}_k , \quad \text{(Eq. 20)}$$

where $\mathbf{J}_k$ is the Jacobian matrix of weighted residuals with m×n components, $J_{ij}=\partial y_i/\partial p_j$; $\mathbf{G}_k$ is the Hessian matrix of weighted residuals with n×n components $G_{jj'}=\partial^2 y_i/(\partial p_j \partial p_{j'})$. The gradient vector of the objective function is expressed as $\mathbf{g}_k=2\cdot\mathbf{J}_k^T\cdot\mathbf{y}_k$.

The Gauss-Newton algorithm premises that the first-order term dominates the second-order term of the Hessian matrix in Eq. 20, which leads to the following approximation:

$$\mathbf{p}_{k+1} = \mathbf{p}_k - \frac{1}{2} \cdot \left[ \mathbf{J}_k^T \cdot \mathbf{J}_k \right]^{-1} \cdot \mathbf{g}_k . \quad \text{(Eq. 21)}$$

In the Levenberg-Marquardt algorithms the second-order term in Eq. 20 is approximated by an n×n diagonal matrix $\lambda_k\cdot\mathbf{D}_k$. $\mathbf{D}_k$ is composed of the diagonal components of $\mathbf{J}_k^T\cdot\mathbf{J}_k$ and its components are given by $D_{jj}=(\mathbf{J}_k^T\cdot\mathbf{J}_k)_{jj}$. $\lambda_k$ is a scalar that is changed during the iterative computation corresponding to the change in the value of the objective function. By introducing $\lambda_k\cdot\mathbf{D}_k$ into Eq. 20, the following expression can be derived:

$$\mathbf{p}_{k+1} = \mathbf{p}_k - \frac{1}{2} \cdot \left[ \mathbf{J}_k^T \cdot \mathbf{J}_k + \lambda_k \cdot \mathbf{D}_k \right]^{-1} \cdot \mathbf{g}_k . \quad \text{(Eq. 22)}$$

After each iteration, $\lambda_k$ is either increased or decreased, depending on the change in the value of the objective function, $S(\mathbf{p})$ (Eq. 14). When $S(\mathbf{p}_{k+1})>S(\mathbf{p}_k)$, $\lambda$ is increased; when $S(\mathbf{p}_{k+1})<S(\mathbf{p}_k)$, $\lambda$ is decreased in the next iterative step. When $\lambda_k$ is large, the inverse matrix in Eq. 22 is forced into being diagonally dominant, so Eq. 22 becomes close to that for the steepest descent method:

$$\mathbf{p}_{k+1} = \mathbf{p}_k - a \cdot \mathbf{g}_k , \quad \text{(Eq. 23)}$$

where $a$ is a constant. On the other hand, as $\lambda_k$ approaches zero, Eq. 22 approaches Eq. 21. Thus the Levenberg-Marquardt method can be viewed as a flexible combination of the steepest-descent method and the Gauss-Newton method.

A description of the robustness of each minimization algorithm is beyond the scope of this paper. It suffices to point out that the parameter vector, $\mathbf{p}_{k+1}$, is searched based on the gradient vector of the objective function, $\mathbf{g}_k$, in the gradient-based algorithms; thus the objective function should be smooth, meaning continuous and differentiable. When the objective function is the sum of squares, the objective function near the global minimum is close to parabolic with elliptical contour lines, which is advantageous to the Newton-type minimization algorithms with quadratic approximation of the objective function. However, searching the global minimum becomes significantly difficult for cases where the topology of the objective function away from the global minimum exhibits multiple local minima or points (including lines) at which the gradient vector become 0 or discontinuous. For those cases, the parameter vector, $\mathbf{p}$, may be stuck in wrong points depending on the initial guess. In addition, the parameter estimation becomes nonunique when multiple parameter combinations produce the same value of the objective function close to that for the global minimum. In other words, it depends on the topology of the objective function whether the inverse problem is well- or ill-posed; this can also be said for the other minimization algorithms searching the optimum parameter set on the objective functions without the gradient vector, $\mathbf{g}$. Therefore, examining the topology of the objective function is of fundamental importance for selecting an appropriate minimization algorithm as well as for knowing the uniqueness of the problem itself. On the other hand, parameter studies of the topologies prior to performing any experiments would provide meaningful information, i.e., whether the inverse problem can be well-posed or how the problem can be well-conditioned by appropriately selecting experimental conditions or

collecting the measurement data. Considering the importance of characterizing the objective function both in selecting the inverse analysis method and in conditioning the inverse problem by appropriate experimental design, the objective functions should preferably be evaluated prior to performing experiments, when theoretical or numerical analysis of the objective function's concavity is feasible [e.g., 23-25].

## Calculation of parameter vector

In inverse analyses based on Newton-type minimization algorithms, the parameter vector, **p**, at each iterative step is derived by solving one of Eqs. 20, 21, or 22. In the mathematical expressions, the parameter vector, **p**, seems to be calculated using the inverse matrix but in practice it is derived by solving algebraic equations without calculating the inverse matrix. At each iterative step, Eqs. 21 and 22 are formulated as linear algebraic equations. The solution of the linear algebraic equation can be derived by solving the problem as is, meaning directly solving the normal equation, or by a QR decomposition of the matrix in the normal equation.

In the normalized form, Eq. 21 for the Gauss-Newton algorithm can be expressed as:

$$\mathbf{J}'^{\mathrm{T}}_{\mathrm{k}} \cdot \mathbf{J}'_{\mathrm{k}} \cdot \Delta\mathbf{p} = \mathbf{J}'^{\mathrm{T}}_{\mathrm{k}} \cdot \mathbf{y}_{\mathrm{k}} \,. \qquad \text{(Eq. 21')}$$

where $\mathbf{J'}_{\mathrm{k}}$ is the weighted Jacobian matrix of the functional model, $z_{\mathrm{i}}$, with m×n components, $J'_{ij}=(1/\sigma_{zi})\cdot(\partial z_i/\partial p_{jj})$, and $\Delta\mathbf{p}=\mathbf{p}_{k+1}-\mathbf{p}_k$. For the Levenberg-Marquardt algorithm, the normal equation can be derived by introducing alternative matrices, $\mathbf{D'}_{\mathrm{k}}$ ($D'_{jj}=(\mathbf{J'}^{\mathrm{T}}_{\mathrm{k}}\cdot\mathbf{J'}_{\mathrm{k}})_{jj}$) and $\mathbf{J''}_{\mathrm{k}}=\mathbf{J'}_{\mathrm{k}}\cdot[\mathbf{D'}^{1/2}_{\mathrm{k}}]^{-1}$, and the vector $\Delta\mathbf{p'}=[\mathbf{D'}^{1/2}_{\mathrm{k}}]\cdot\Delta\mathbf{p}$ and rewriting Eq. 22:

$$\left(\mathbf{J}''^{\mathrm{T}}_{\mathrm{k}} \cdot \mathbf{J}''_{\mathrm{k}} + \lambda_{\mathrm{k}} \cdot \mathrm{I}\right)\cdot \Delta\mathbf{p}' = \mathbf{J}''^{\mathrm{T}}_{\mathrm{k}} \cdot \mathbf{y}_{\mathrm{k}} \,, \qquad \text{(Eq. 22')}$$

where **I** is the identity matrix. Further introducing $\mathbf{J'''}^{\mathrm{T}}_{\mathrm{k}}=[\mathbf{J''}^{\mathrm{T}}_{\mathrm{k}} \mid \lambda_{\mathrm{k}}^{1/2}\cdot\mathbf{I}]$ and $\mathbf{y'}^{\mathrm{T}}_{\mathrm{k}}=[\mathbf{y}_{\mathrm{k}}^{\mathrm{T}} \mid \mathbf{0}]$, Eq. 22' can be rewritten as:

$$\mathbf{J}'''^{\mathrm{T}}_{\mathrm{k}} \cdot \mathbf{J}'''_{\mathrm{k}} \cdot \Delta\mathbf{p}' = \mathbf{J}'''^{\mathrm{T}}_{\mathrm{k}} \cdot \mathbf{y}'_{\mathrm{k}} \,, \qquad \text{(Eq. 22'')}$$

where $\mathbf{J'''}_{\mathrm{k}}$ is a matrix with (m+n)×n components; $\mathbf{y'}_{\mathrm{k}}$ is a vector with m+n components involving vector $\mathbf{y}_{\mathrm{k}}$ from the 1-st to m-th components and zero in the other.

When applying the QR decomposition to the above normal equations, Eqs. 21' and 22'' are reduced to the following equations:

$$\mathbf{J}'_{\mathrm{k}} \cdot \Delta\mathbf{p} = \mathbf{y}_{\mathrm{k}} \,, \qquad \text{(Eq. 21'')}$$

$$\mathbf{J}'''_{\mathrm{k}} \cdot \Delta\mathbf{p}' = \mathbf{y}'_{\mathrm{k}} \,. \qquad \text{(Eq. 22''')}$$

For accurate computation of the parameter vector, $\Delta\mathbf{p}$, the condition numbers of the matrices on the left hand sides of Eqs. 21', 22'', 21'', and 22''' should be taken into consideration [e.g., 26]. The condition number of a matrix can be cited as the measure of to what extent the inverse problem is well- or ill-posed. The condition number associated with the linear equation $\mathbf{A}\cdot\mathbf{x}=\mathbf{b}$ is given by the following expression:

$$\kappa(\mathbf{A}) = \left|\frac{\mu_{\max}(\mathbf{A})}{\mu_{\min}(\mathbf{A})}\right|, \qquad \text{(Eq. 24)}$$

where $\kappa(\mathbf{A})$ is the condition number of a matrix; $\mu_{\max}$ and $\mu_{\min}$ are maximal and minimal singular values, respectively, of **A**. From the viewpoint of numerical computation, the condition number could be thought of as the rate at which the solution, **x**, will change with respect to a change in **b**. Thus, if the condition number is large, even a small error in **b** may cause a large error in **x**. On the other hand, if the condition number is small then the error in **x** will not be much bigger than the error in **b**. Accordingly, a problem with a low condition number is said to be well-conditioned, while a problem with a high condition number is said to be ill-conditioned. For example, if the number of parameters is 2 and the weighted Jacobian matrices in Eqs. 21', 22'', 21'', and 22''' are derived as follows:

$$\mathbf{J}^{\mathrm{T}} = \begin{bmatrix} \cdots \text{in orders of magnitude of } 10^{5} \cdots \\ \cdots \text{in orders of magnitude of } 10^{0} \cdots \end{bmatrix} \begin{matrix} \leftarrow \text{row for parameter } p_1 \\ \leftarrow \text{row for parameter } p_2 \end{matrix},$$

the condition numbers for $\mathbf{J}^{\mathrm{T}}\cdot\mathbf{J}$ and $\mathbf{J}$ result in orders of $10^{10}$ and $10^{5}$, respectively. Accordingly, the QR decomposition working with $\mathbf{J}$ is advantageous. In addition, the roundoff errors due to singularity could be lowered by the QR decomposition rather than directly solving the normal equation. The condition numbers of $\mathbf{J}^{\mathrm{T}}\cdot\mathbf{J}$ and $\mathbf{J}$ become small when the differences in the orders of magnitudes of component values are small. Therefore, it should be meaningful for knowing or conditioning the weighted Jacobian matrix to examine its component values.

As mentioned in the previous section, $\lambda$ is decreased and close to zero near the minima. Thus Eqs. 22" and 22"' are forced into being Eqs. 21' and 21", respectively. Accordingly, the quality of computing the parameter vector near the minima could be known by evaluating $\mathbf{J'}^{\mathrm{T}}\cdot\mathbf{J'}$ or the weighted Jacobian matrix $\mathbf{J'}$.

## Sensitivity analysis

For characterizing the weighted Jacobian matrix, an additional consideration is described here in light of the sensitivity analysis.

Substituting the weighted residual, Eq. 15, into the Jacobian matrix $\mathbf{J}$, the components of the weighted Jacobian matrix are expressed as:

$$\mathbf{J}' = \begin{bmatrix} \frac{1}{\sigma_{z_1}}\cdot\frac{\partial z_1}{\partial p_1} & \cdots & \frac{1}{\sigma_{z_1}}\cdot\frac{\partial z_1}{\partial p_n} \\ \vdots & & \vdots \\ \frac{1}{\sigma_{z_m}}\cdot\frac{\partial z_m}{\partial p_1} & \cdots & \frac{1}{\sigma_{z_m}}\cdot\frac{\partial z_m}{\partial p_n} \end{bmatrix}, \qquad \text{(Eq. 25)}$$

where the components of the weighted Jacobian matrix $\mathbf{J'}$ are the partial derivatives of the functional model, $z(p)$, scaled by the standard deviation of the measurement error, $\sigma_z$, and $\partial z/\partial p$ is referred to as the sensitivity coefficient or traditional sensitivity coefficient.

While the sensitivity coefficients are often evaluated to examine system responses to perturbations of parameters, they inherit fundamental information on the properties of matrices $\mathbf{J}^{\mathrm{T}}\cdot\mathbf{J}$ and $\mathbf{J}$ as seen in Eq. 25, more precisely, the singularities of the matrices. For an extreme example, if the sensitivities of measurement data to one parameter are all zero, the matrices $\mathbf{J}^{\mathrm{T}}\cdot\mathbf{J}$ and $\mathbf{J}$ become singular and their inverse matrices cannot be defined from a mathematical viewpoint. In addition, the condition numbers of the matrices become infinite; and thus estimation of the non-sensitive parameter becomes unstable in numerical computation.

Therefore, the sensitivities should be increased if possible; and thus sensitivity analysis prior to performance of the actual experiment has important consequences. In fact, sensitivity analysis has been conducted for the purpose of investigating appropriate test methods or experimental conditions to obtain parameter-sensitive data [e.g., 18-30]. If the weighted sensitivity coefficients for different parameters are significantly different in their orders of magnitude, conditioning the weighted Jacobian matrix is required for reducing the condition number of $\mathbf{J}^{\mathrm{T}}\cdot\mathbf{J}$ or $\mathbf{J}$ as described in the next section.

For the sensitivity analysis, several sensitivity coefficients are available.

In order to compare the sensitivities of the system responses to parameters with different units, the sensitivity coefficients in Eq. 25 are scaled by the standard deviations of both the parameters of interest, $\sigma_{pj}$, and the measurement data, $\sigma_{zi}$, as follows [e.g., 21,25]:

$$S_{ij} = \frac{\sigma_{p_j}}{\sigma_{z_i}}\cdot\frac{\partial z_i}{\partial p_j}. \qquad \text{(Eq. 26)}$$

The difficulty often faced in sensitivity analysis using Eq. 26 is the definition of the standard deviation of the parameters, $\sigma_{pj}$. When values of the parameter of interest are evaluated by separate experiments or their standard deviations are known, calculation of Eq. 26 is possible. However, assumptions should be

made about the standard deviations of the parameter values when this statistical information about the parameter values is not available. This is a typical situation encountered when estimating values of geological and geotechnical materials' properties, determining the values of parameters included in constitutive law, or evaluating changes in parameter values with respect to changes in experimental conditions.

For prior sensitivity analysis, other types of sensitivity coefficients, i.e., the traditional sensitivity, normalized sensitivity and logarithmic sensitivity coefficients, have been used in the field of subsurface hydrology as summarized in Kabala [26]. The traditional sensitivity coefficient is the partial derivative of the functional model without scaling and is expressed as $\partial z/\partial p$. As seen in Eqs. 19 through 23 and Eq. 25, the traditional sensitivity coefficients are calculated at each iterative step in the gradient-based iterative minimization algorithms. The traditional sensitivity coefficient was also adopted to examine the effective experimental design and data sampling for one-dimensional advection-dispersion experiments by Knopman and Voss [27]. The normalized sensitivity coefficient was introduced into the field of subsurface hydrology by McElwee [28] according to Kabala [26] and expressed as $p\cdot(\partial z/\partial p)$. The normalized sensitivity coefficient is a variant of the traditional sensitivity coefficient. The normalized sensitivity coefficient is the traditional sensitivity coefficient scaled by the parameter of interest; and thus the influence of one parameter on the system response can be compared with the influence of another. The normalized sensitivity coefficient has been used in the dimensionless form by further scaling it by a reference value for measurement, such as the initial pulse in permeability tests [e.g., 29,30]. The scaled normalized sensitivity coefficient is expressed as $(p/z_0)\cdot(\partial z/\partial p)$; where $z_0$ is the reference value for the measurement data. The logarithmic sensitivity is defined as the measure of the influence that a fractional change in the parameter has on fractional changes in the output and is expressed as $(p/z)\cdot(\partial z/\partial p)$. The logarithmic sensitivity is similar to or can be viewed as a generalized form of the sensitivity coefficient defined by Eq. 26 in the light of scaling. While Eq. 26 measures the influence of the coefficient of variance (CV) of a parameter on the CV for a system response, the logarithmic sensitivity measures the influence that a relative change in a parameter has on the relative change in a system response. Although both the logarithmic sensitivity coefficient and the sensitivity coefficient defined by Eq. 26 can compare system responses with different units with respect to one or more parameters, which is not possible with the other sensitivity coefficients, the logarithmic sensitivity coefficient has an advantage over the sensitivity coefficient defined by Eq. 26 in that the logarithmic sensitivity coefficient can be calculated even when the statistical information of the parameters is not available. However, the logarithmic sensitivity coefficient may not be suitable when the functional model reaches zero or increases from zero because the logarithmic sensitivity coefficient becomes infinite in such cases.

In the inverse analyses based on the gradient-based algorithms, the traditional sensitivity coefficients for each measurement time and/or point are calculated at each iterative step as seen in Eq. 25. Thus, direct evaluation of the traditional sensitivity coefficient weighted by the standard deviation of the measurement error (Eq. 25) would be useful in examining an experiment performed with a specific testing material and experimental condition. However, sensitivity analysis with dimensionality requires an enormous computational cost to draw a general idea for experimental design corresponding to various testing materials. Accordingly, sensitivity analysis that works with sensitivity coefficients without dimensionality, namely the scaled-normalized sensitivity coefficient or the logarithmic sensitivity coefficient, would be efficient when a general idea of the feasibility of a new test and the characteristics of the weighted Jacobian matrix are being drawn from the sensitivity analysis.

## Characterization of weighted Jacobian matrix

Using the scaled normalized sensitivity coefficient, the weighted Jacobian matrix **J**' can be expressed as:

$$\mathbf{J}' = \begin{bmatrix} \frac{1}{\sigma_{z_1}} \cdot \frac{z_0}{p_1} \cdot \left( \frac{p_1}{z_0} \cdot \frac{\partial z_1}{\partial p_1} \right) & \cdots & \frac{1}{\sigma_{z_1}} \cdot \frac{z_0}{p_n} \cdot \left( \frac{p_n}{z_0} \cdot \frac{\partial z_1}{\partial p_n} \right) \\ \vdots & & \vdots \\ \frac{1}{\sigma_{z_m}} \cdot \frac{z_0}{p_1} \cdot \left( \frac{p_1}{z_0} \cdot \frac{\partial z_m}{\partial p_1} \right) & \cdots & \frac{1}{\sigma_{z_m}} \cdot \frac{z_0}{p_n} \cdot \left( \frac{p_n}{z_0} \cdot \frac{\partial z_m}{\partial p_n} \right) \end{bmatrix}, \qquad \text{(Eq. 25')}$$

where the traditional sensitivity coefficients in Eq. 25 are replaced with the normalized sensitivity coefficient scaled by the reference value, $z_0$, and the parameters of interest. In Eq. 25', each component is expressed by multiplying the scaled normalized sensitivity coefficient by the inverses of the parameter of interest and $\sigma_{zi}/z_0$. When a measurement with a fixed accuracy, e.g., a concentration measurement by an ion-selective electrode, can be assumed, $\sigma_{zi}/z_0$ becomes constant and identical to the coefficient of variance (CV) for measurement.

When the coefficient of variance (CV) for measurement changes with respect to a change in the measurement value, e.g., a concentration measurement by chromatography, Eq. 25 can be rewritten using the logarithmic sensitivity coefficients as follows:

$$\mathbf{J}' = \begin{bmatrix} \frac{1}{\sigma_{z_1}} \cdot \frac{z_1}{p_1} \cdot \left( \frac{p_1}{z_1} \cdot \frac{\partial z_1}{\partial p_1} \right) & \cdots & \frac{1}{\sigma_{z_1}} \cdot \frac{z_1}{p_n} \cdot \left( \frac{p_n}{z_1} \cdot \frac{\partial z_1}{\partial p_n} \right) \\ \vdots & & \vdots \\ \frac{1}{\sigma_{z_m}} \cdot \frac{z_m}{p_1} \cdot \left( \frac{p_1}{z_m} \cdot \frac{\partial z_m}{\partial p_1} \right) & \cdots & \frac{1}{\sigma_{z_m}} \cdot \frac{z_m}{p_n} \cdot \left( \frac{p_n}{z_m} \cdot \frac{\partial z_m}{\partial p_n} \right) \end{bmatrix}, \qquad \text{(Eq. 25")}$$

where each component is expressed by multiplying the logarithmic sensitivity coefficient by the inverses of the parameter of interest and $\sigma_{zi}/z_i$. $\sigma_{zi}/z_i$ is the coefficient of variance (CV) for measurement in this case.

As seen in both Eq. 25' and 25", the condition numbers of the Jacobian **J**' are affected by the coefficient of variance (CV) for measurement as well as the values of the parameters of interest and the sensitivity coefficients. However, the coefficient of variance (CV) has different meanings in Eq. 25' and 25" and the sensitivity coefficients used in each expression are also different. This means that the way of characterizing the weighted Jacobian matrix should be selected depending on the type of coefficient of variance (CV) for measurement. Specifically, when the coefficient of variance (CV) for measurement is constant for all measurement values, the weighted Jacobian matrix should be examined by the normalized sensitivity coefficient; when the coefficient of variance (CV) for measurement depends on the measurement value, the logarithmic sensitivity coefficient is appropriate. It should be noted that Eqs. 25' and 25" are used for characterization of the weighted Jacobian matrix, Eq. 25; for calculation of the parameter vector in the inverse analysis, the weighted Jacobian matrix is calculated by Eq. 25.

In the above, it was shown that the components of the weighted Jacobian matrix can be decomposed into the sensitivity coefficient, the coefficient of variance (CV) for measurement and the parameter of interest. Thus, the importance of each measurement point in time and/or space can be evaluated by examining its sensitivity coefficient and CV assuming the values of the parameter of interest. As shown, the sensitivity coefficient without dimensionality is more suitable than those requiring dimensioned parameters for general characterization of the weighted Jacobian matrix. In addition, the scaled normalized and logarithmic sensitivity coefficients can be calculated without the dimensioned parameter. Furthermore, the coefficient of variance (CV) for measurement can be known or supposed in selecting the measurement device. Accordingly, the property of the weighted Jacobian matrix, more precisely the condition number defined as Eq. 24, can be evaluated assuming the values of the parameters of interest.

In Eq. 25' and 25", the parameter values are unknown prior to the experiments. However, differences in the orders of magnitude between each parameter value can be estimated to some extent. When the differences in the orders of magnitude between each parameter value are significant, meaning that the order of magnitude of a specific parameter value, $p_j$, is significantly smaller than those of the other

parameters, the condition number become large as mentioned in the previous section using Eq. 24. We note in passing that, when the measurement values reach zero or start from zero, the weighted Jacobian matrix should be characterized by the scaled normalized sensitivity coefficient rather than the logarithmic sensitivity coefficient, even if the coefficient of variance (CV) for measurement varies with the measurement value. In such a case, the CV for measurement should be approximated as the CV for measurement with a constant accuracy. Otherwise, the collection of measurement data with values close to zero should be avoided.

## Conditioning of weighted Jacobian matrix

As described in Eq. 25' and 25", a well-conditioned weighted Jacobian matrix can not be ensured only by sensitivity coefficient values; the condition number is also affected by the coefficient of variance (CV) for measurement as well as the value of the parameter of interest. When the conditional number is expected to become large, conditioning of the weighted Jacobian matrix is needed. For example, this might be done by collecting parameter-sensitive data and/or decreasing the coefficient of variance (CV) for measurement, i.e., increasing the measurement accuracy by calibrating the measurement device more sensitively to the ranges over which the data is measured, or by using a more precise measurement device or method. However, when the differences in the orders of magnitude of the parameter values are significant, the condition number inevitably becomes large. In such a case, additional treatment of the weighted Jacobian matrix **J**' would lower the condition number. One way of lowering the condition number is to use $\log(p_j)$ as an alternative parameter to $p_j$; where $p_j$ is the parameter having a significantly smaller value than the other parameters. In this treatment, the components for the parameter $p_j$ in the weighted Jacobian matrix are replaced with those for $\log(p_j)$ and minimization of the objective function is performed with the rearranged weighted Jacobian matrix.

The traditional sensitivity coefficient for $\log(p_j)$ can be calculated by numerical differentiation of the functional model as performed by Finsterle and Persoff [18]. However, for the functional models defined as analytical solutions, we introduce the traditional sensitivity coefficient for $\log(p_j)$ as follows:

$$\frac{\partial z}{\partial \log(p_i)} = \frac{p_i}{\log(e)} \cdot \frac{\partial z}{\partial p_i} . \qquad \text{(Eq. 27)}$$

As indicated by Eq. 27, the traditional sensitivity coefficient for $\log(p_j)$ can be derived by dividing the normalized sensitivity coefficient by $\log(e)$=0.43… . Therefore, calculation of the traditional sensitivity coefficient is more straightforward than numerical differentiation for the functional model defined as the analytical solution. Substituting Eq. 27 into Eq. 25, the weighted Jacobian matrix can be written as follows:

$$\mathbf{J}' = \begin{bmatrix} \frac{1}{\sigma_{z_1}} \cdot \frac{\partial z_1}{\partial p_1} & \cdots & \frac{1}{\sigma_{z_1}} \cdot \frac{p_j}{\log(e)} \cdot \frac{\partial z_1}{\partial p_j} & \cdots & \frac{1}{\sigma_{z_1}} \cdot \frac{\partial z_1}{\partial p_n} \\ \vdots & & \vdots & & \vdots \\ \frac{1}{\sigma_{z_m}} \cdot \frac{\partial z_m}{\partial p_1} & \cdots & \frac{1}{\sigma_{z_m}} \cdot \frac{p_j}{\log(e)} \cdot \frac{\partial z_m}{\partial p_j} & \cdots & \frac{1}{\sigma_{z_m}} \cdot \frac{\partial z_m}{\partial p_n} \end{bmatrix} . \qquad \text{(Eq. 25"')}$$

The redefined weighted Jacobian matrix should be further examined by Eq. 25' or 25" depending on the coefficient of variance (CV) for measurement. When the condition number is still large, the other parameter with a small order of magnitude might be transformed into a base-10 logarithmic value. Depending on the orders of magnitude of the parameter values, all components in the weighted Jacobian matrix in Eq. 25 might be defined as base-10 logarithmic parameters.

When measurement data with different units are obtained in a single experiment, the logarithmic sensitivity would be appropriate. However, the measurement data in the single-reservoir radial diffusion test being addressed in this paper is only the reservoir concentration; thus the normalized sensitivity coefficient scaled by a reference value can also be applied. The method of characterization of the

weighted Jacobian matrix is selected depending on the coefficient of variance (CV) for measurement. In the following, provided that the concentration is measured with a fixed accuracy, the normalized sensitivity coefficient scaled by a reference value is adopted for evaluation of the single-reservoir radial diffusion test for a cylindrical specimen.

## NUMERICAL EXAMINATION

In diffusion experiments, the testing materials and tracers are first selected or given. Accordingly, the diffusion experiment should be designed appropriately for both the testing material and the tracer. The experimental conditions, such as the dimensions of the specimen and reservoir, should be selected to maximize the measurement resolution and the accuracy of the test interpretation while minimizing the experimental duration.

The experimental duration is an important factor affecting the feasibility of the experiment, as the experimental duration has been a main concern in selecting experimental methods for 1D laboratory diffusion experiments [e.g., 12-14]. In the previous section, the analytical solution to the single-reservoir radial diffusion test for a cylindrical specimen was derived in the dimensionless form so as to compare the experimental durations of different experimental conditions, i.e., the source reservoir volume, for a specimen with certain diffusive and adsorptive properties and dimensions. On the other hand, inverse analysis of transient data is needed when the experimental duration is very long. For successful parameter estimation by inverse analysis, prior sensitivity analysis is necessary.

In order to examine the dependences of both the experimental duration and the sensitivity on the experimental conditions, a series of numerical examinations are conducted using the analytical solution in this section.

### Transient variation of reservoir concentration

Type curves of transient variations of solute concentrations in the source reservoir were calculated by Eq.10 setting $\rho$=1 (Fig. 2). The dimensionless reservoir volume, $\beta_r$, was varied from $10^{-2}$ to $10^{1}$ to cover various experimental conditions. As a whole, the solute concentrations reach the equilibrium state before $\tau$=1. Comparing the equilibrium concentrations between different values of $\beta_r$, the concentration tends to increase as the value of $\beta_r$ increases. In other words, no drastic change in the reservoir concentration is expected when the value of $\beta_r$ is set too high. In that case, it might be difficult to accurately measure small variations in the concentrations that depend on the resolution of the solute detection. Considering the above, a small $\beta_r$ is advantageous for measuring the transient variations of solute concentration in the source reservoir.

### Sensitivities of reservoir concentration to $D_e$ and $\alpha$

The normalized sensitivity coefficients of the reservoir concentration can be evaluated by the following expressions coupled with Eq. 10 for the effective diffusion coefficient and capacity factor:

$$\frac{D_e}{C_0}\cdot\frac{\partial C}{\partial D_e}=\tau\cdot\frac{\partial c}{\partial \tau}, \qquad \text{(Eq. 28)}$$

$$\frac{\alpha}{C_0}\cdot\frac{\partial C}{\partial \alpha}=\tau\cdot\frac{\partial c}{\partial \tau}+\beta_r\cdot\frac{\partial c}{\partial \beta_r}, \qquad \text{(Eq. 29)}$$

where the normalized sensitivity coefficients are scaled by the initial concentration in the source reservoir, $C_0$. In the simulations, the values for $\beta_r$ were varied as in the previous section.

Transient variations in the sensitivities to the effective diffusion coefficient, $D_e$, calculated by Eq. 28 are shown in Fig. 3. As a whole, the sensitivity to $D_e$ gradually increases as time elapses and decreases after

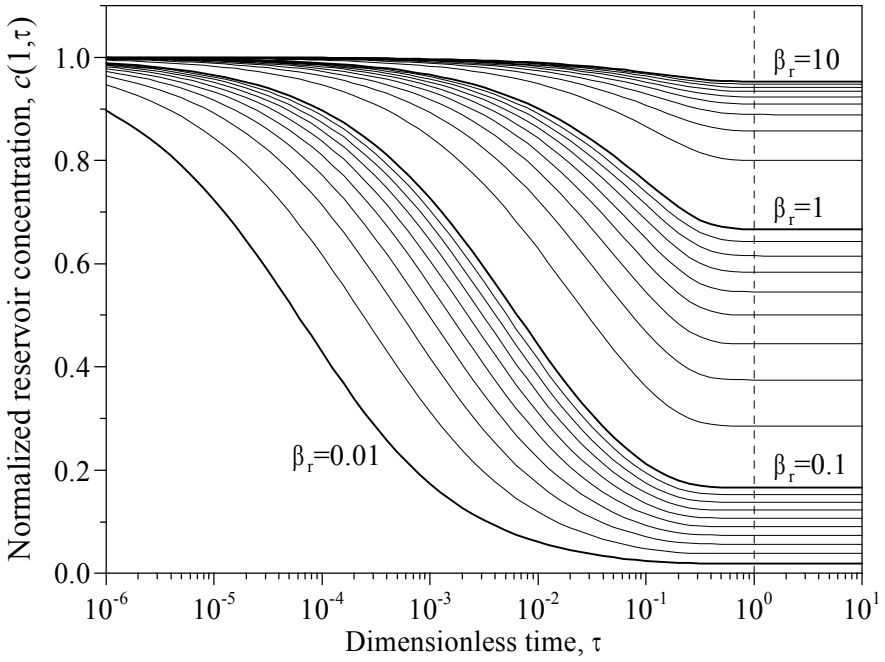


Fig. 2. Transient variation of normalized reservoir concentration.

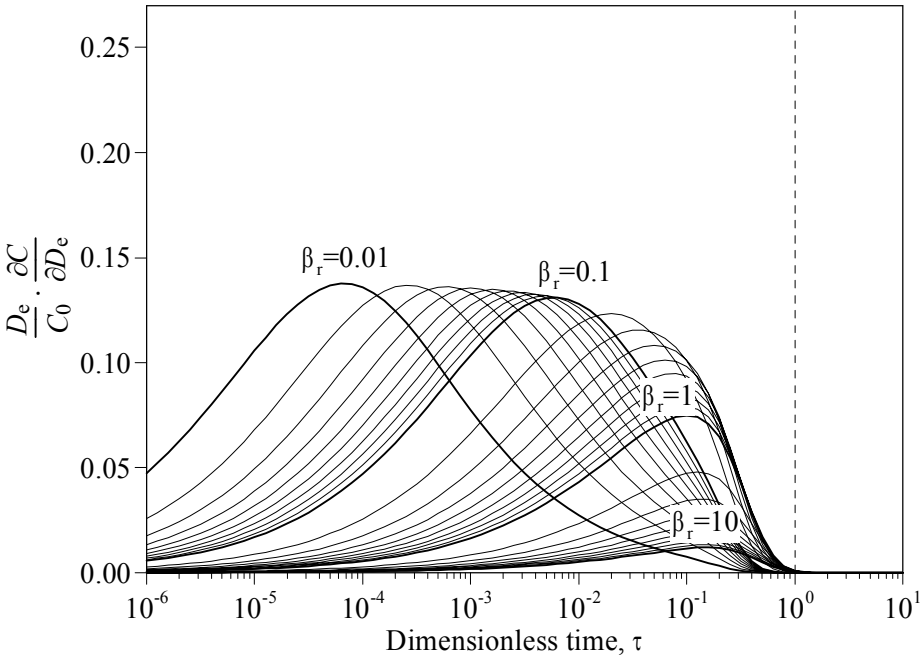


Fig. 3. Transient variation of normalized sensitivity coefficient of reservoir concentration to $D_e$ scaled by the initial reservoir concentration, $C_0$.

the maximum has been reached. The smaller the value of $\beta_r$, the earlier the maximum sensitivities appear, with larger absolute values. At the equilibrium state, the sensitivities to $D_e$ become zero as reasoned by Eqs. 10 and 28.

On the other hand, the sensitivities to the capacity factor, $\alpha$, calculated by Eq. 29 showed different trends (Fig. 4). The time series variation of the sensitivity to $\alpha$ is composed of those for the transient and equilibrium states. In cases where $\beta_r$ is less than $10^{-1}$, the sensitivity coefficients have almost identical

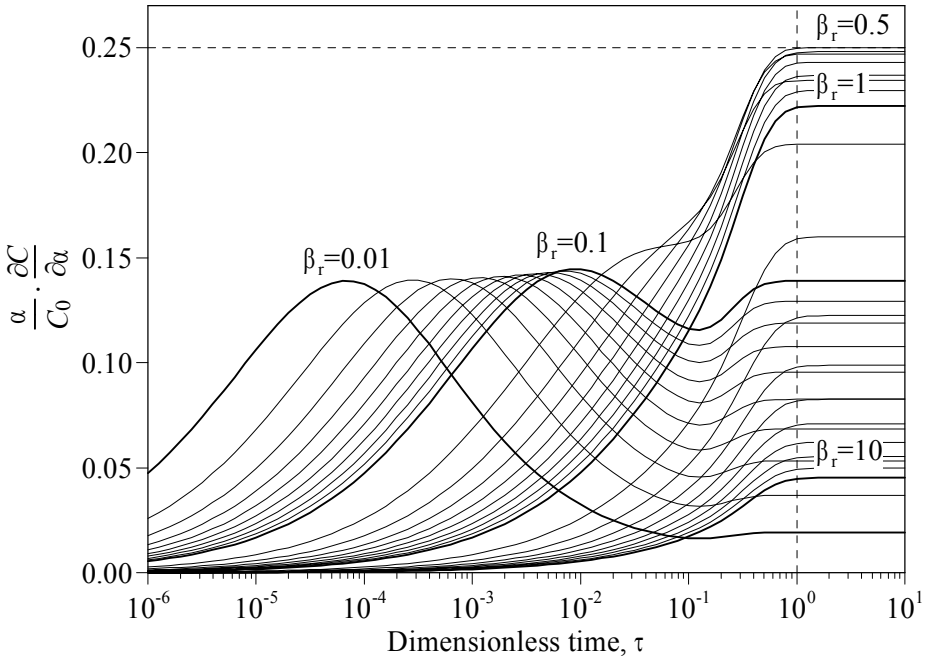


Fig. 4. Transient variation of normalized sensitivity coefficient of reservoir concentration to α scaled by the initial reservoir concentration, $C_0$.

values at their maxima, while those for the equilibrium state vary depending on the values of $\beta_r$. In addition, the maximum sensitivity during the transient phase is larger than that for the equilibrium state. As the values of $\beta_r$ become larger than $10^{-1}$, the sensitivity to $\alpha$ becomes large as time elapses and shows its maximum value at the equilibrium state. The largest absolute value of sensitivity to $\alpha$ is -0.25 for the case with $\beta_r$=0.5 as calculated using Eqs. 12 and 29. For the cases with $\beta_r$ larger than 0.5, the maximum sensitivity to $\alpha$ tends to be small as the value of $\beta_r$ becomes large. As a whole, the normalized sensitivity coefficients to $\alpha$ tend to have large values during the late portion of the transient state.

## DISCUSSION

In the previous section, it was shown that the dimensionless reservoir volume, $\beta_r$, affects both the experimental duration and the sensitivities of the reservoir concentration. In this section, the experimental design for expediting experiments and the characteristics of the Jacobian matrix, **J**, and the matrix, $\mathbf{J}^T \cdot \mathbf{J}$, are discussed.

### Experimental duration

As indicated by Eq. 7, regardless the experimental conditions, the experimental duration is inversely proportional to the effective diffusion coefficient, $D_e$, and proportional to the capacity factor, $\alpha$. This means that the experimental duration is affected by both $D_e$ and $\alpha$ and tends to be long when $D_e$ and $\alpha$ become small and large, respectively. The distribution coefficient, $K_d$, is implicitly included in the capacity factor, $\alpha$ ($\varepsilon+\rho_s \cdot K_d$), and tends to be larger when the tracer is more sorptive. In other words, the more sorptive the tracer, the larger the value of $\alpha$ and the longer the duration of the experiment.

On the other hand, the use of a sorptive tracer, giving a large $\alpha$, also makes a difference in obtaining drastically changing concentration data as shown in Fig. 2. If $\beta_r$ becomes small due to the use of a sorptive tracer (Eq. 9), relatively large variations in the solute concentrations can be expected over a shorter experimental period than for the cases with a large $\beta_r$. This would be helpful for terminating the measurement during the transient state if the values of the parameters can be inversely determined from

the transient data. However, depending on experimental conditions other than the tracer property, the experiment may last long in spite of one's expectations, even if a strongly sorptive tracer is used. This is because $\beta_r$ includes other parameters, such as the dimensions of the specimen and reservoir. Accordingly, it is important to pertinently select the dimensions of the specimen and reservoir so as to make $\beta_r$ small.

The capacity factor, $\alpha$, is unknown prior to performance of the experiments. However, its minimum value can be estimated if the porosity is known and zero sorption is assumed. In addition, the maximum value of the capacity factor can be inferred when the distribution coefficient, $K_d$, and the bulk density, $\rho_b$, as well as the porosity, $\varepsilon$, of the testing material are known or supposed from similar materials. Based on the minimum and maximum values of the capacity factor, the maximum and minimum values of $\beta_r$ can be approximated by Eq. 9, which enables comparison of the maximum and minimum experimental durations for different experimental conditions as shown in Fig. 2. Thus, when selecting the experimental conditions, it is recommended to approximate the value of the dimensionless reservoir volume, $\beta_r$, by using the porosity, density and distribution coefficient of the testing material if they are available.

## Parameter sensitivity and weighted Jacobian matrix

As shown by Eqs. 12 and 13, the capacity factor, $\alpha$, and/or the distribution coefficient, $K_d$, can be estimated from the equilibrium concentration separately from the transient analysis. However, the actual experimental duration for establishment of the equilibrium state might be impractically long when the effective diffusion coefficient of the specimen, $D_e$, is very small. The practical way of parameter estimation in such a case would be to inversely determine the values of $D_e$ and $\alpha$ from the measured concentrations during the transient phase. If the Newton-type minimization algorithms using the objective function defined as the sum of the squared residuals between the measured and calculated concentrations are adopted, parameter-sensitive data is necessary as discussed using Eqs. 20 through 25"'.

When $\beta_r$ is greater than $10^{-1}$, the sensitivity to $D_e$ tends to be relatively small as the value of $\beta_r$ becomes large, while that to $\alpha$ tends to be large (Fig. 3 and 4). On the other hand, when $\beta_r$ is less than $10^{-1}$, the sensitivities to both the effective diffusion coefficient, $D_e$, and the capacity factor, $\alpha$, are almost equally large until the maximum sensitivities appear and almost same maximum values are shown for different values of $\beta_r$. Accordingly, a small $\beta_r$ is advantageous for obtaining measurement data that is almost equally sensitive to both the effective diffusion coefficient and the capacity factor.

As a whole, the sensitivity can be seen in all the simulated cases, which would satisfy the condition for the existence of the inverse matrices in Eqs. 20 through 22. However, the quality of the parameter estimation might not be ensured depending on the condition numbers of the matrices in Eqs. 21', 22", 21", and 22"'. Here, the condition numbers of those matrices are discussed again focusing on the matrix $\mathbf{J'}^{T}\cdot\mathbf{J'}$ and the Jacobian $\mathbf{J}$' in the inverse analysis of the radial diffusion tests. Now that the scaled normalized sensitivity coefficient is available, the weighted Jacobian matrix $\mathbf{J}$' (Eq. 25") for the diffusion experiment can be expressed as:

$$\mathbf{J}' = \begin{bmatrix} \frac{1}{\sigma_{C_1}}\cdot\frac{C_0}{D_e}\cdot\left(\frac{D_e}{C_0}\cdot\frac{\partial C_1}{\partial D_e}\right) & \frac{1}{\sigma_{C_1}}\cdot\frac{C_0}{\alpha}\cdot\left(\frac{\alpha}{C_0}\cdot\frac{\partial C_1}{\partial \alpha}\right) \\ \vdots & \vdots \\ \frac{1}{\sigma_{C_i}}\cdot\frac{C_0}{D_e}\cdot\left(\frac{D_e}{C_0}\cdot\frac{\partial C_i}{\partial D_e}\right) & \frac{1}{\sigma_{C_i}}\cdot\frac{C_0}{\alpha}\cdot\left(\frac{\alpha}{C_0}\cdot\frac{\partial C_i}{\partial \alpha}\right) \\ \vdots & \vdots \\ \frac{1}{\sigma_{C_m}}\cdot\frac{C_0}{D_e}\cdot\left(\frac{D_e}{C_0}\cdot\frac{\partial C_m}{\partial D_e}\right) & \frac{1}{\sigma_{C_m}}\cdot\frac{C_0}{\alpha}\cdot\left(\frac{\alpha}{C_0}\cdot\frac{\partial C_m}{\partial \alpha}\right) \end{bmatrix},$$

where $C_i$ and $\sigma_{Ci}$ are the i-th measured concentration and the standard deviation of the measurement error.

As shown in Figs. 3 and 4, the scaled normalized sensitivity coefficients to $D_e$ and $\alpha$ are in the minus one order of magnitude. Providing that the values of $\sigma_{Ci}/C_0$ are minus three orders of magnitude, the orders of

magnitude of the component values for each parameter depend on the parameter values themselves. For this example, the above expression can be approximately written as:

$$\mathbf{J'}^{\mathrm{T}} = 10^{2} \cdot \begin{bmatrix} \cdots \text{orders of magnitude of } 1/D_{\mathrm{e}} \text{ value} \cdots \\ \cdots \text{orders of magnitude of } 1/\alpha \text{ value} \cdots \end{bmatrix} \begin{matrix} \leftarrow \text{row for } D_{\mathrm{e}} \\ \leftarrow \text{row for } \alpha \end{matrix} .$$

In general, the orders of magnitude of $D_e$ values are significantly smaller than those of $\alpha$ for geological and geotechnical materials, and differences in the orders of magnitude between $D_e$ and $\alpha$ values would be around ten. Supposing that the values for $D_e$ and $\alpha$ are $10^{-10}$ and $10^{0}$, respectively, the condition numbers of $\mathbf{J'}^{\mathrm{T}} \cdot \mathbf{J'}$ and $\mathbf{J'}$ can be calculated as $10^{20}$ and $10^{10}$, respectively (Eqs. 24 through 25"'). In addition, since the values of the components for $\alpha$ in the weighted Jacobian matrix are significantly smaller than those for $D_e$, computation of the $\alpha$ value becomes susceptible to roundoff errors and perturbations in values on the right hand side of Eqs. 21', 22", 21" and 22"', i.e., the measurement error. When the roundoff error is significant, the parameter estimation might be improved by working with the weighted Jacobian matrix defined by $\log(D_e)$ or both $\log(D_e)$ and $\log(\alpha)$ as alternative parameters. If the condition number is successfully lowered, the error in the parameter values will not be much larger than the error in the measurement.

## Experimental conditions

As already mentioned, $\beta_r$ is the key parameter for obtaining drastically changing concentration data and parameter-sensitive data with respect to both the effective diffusion coefficient and the capacity factor. $\beta_r$ includes three adjustable parameters, i.e., the reservoir volume and the radius and length of the specimen (Eq. 9). Thus, in order to expedite the experiment and obtain parameter-sensitive data, the dimensions of these adjustable parameters should be selected so as to make the value of $\beta_r$ small. Another adjustable parameter prior to commencement of experiments is the initial concentration in the source reservoir, $C_0$, which directly affects the measurement accuracies. For selection of these adjustable parameters, the general considerations are described as follows:

- It is better to keep the specimen radius short because the actual experimental time is proportional to the square of the specimen radius (Eq. 7). If the specimen radius is too large, $t$ becomes long for a certain value of $\tau$, which is equal to the extension of the transient phase.
- The reservoir volumes should not be set too small when the reservoir solution is sampled for concentration measurement. This is because the loss in solution volume by sampling enlarges the discrepancies between the actual experiments and the analytical models assuming constant volumes for the reservoir during experiments.
- The length of the specimen can be set to be arbitrarily large without any theoretical limitations. However, a long specimen enlarges the reservoir volumes surrounding the specimen, which might be a disadvantage for keeping the solute concentration constant in the reservoir. However, this problem would be overcome by stirring the solution or by other treatment.
- The magnitude of the change in the solute concentration becomes small when the value of $\beta_r$ is large (see flat line in Fig. 2). In such a case, it might be difficult to accurately measure small variations in concentrations, depending on the type of concentration measurement and its resolution, which should be considered in selecting the reservoir volume and the measurement device.
- The initial concentration in the source reservoir, $C_0$, is proportional to the magnitude of the measurement data. Thus its value should be set appropriately, taking the measurement resolution and measurable range of the concentration into consideration.

## CONCLUSION

Evaluation of the directional diffusivities and adsorptive properties of natural barrier materials is of fundamental importance in the design and assessment of geological disposal of hazardous contaminants including radioactive nuclear wastes.

In order to facilitate estimation of the anisotropic diffusivity considered as a 2D tensor, a single-reservoir radial diffusion test for a cylindrical specimen was proposed in this study. The proposed test would enable doubly testing a cylindrical specimen, by both radial and 1D diffusion tests, which would provide better understanding of the directional diffusivity of materials with geometric orientation of pore structures, especially preferentially layered sediments.

The feasibility of the proposed radial diffusion test was examined from the viewpoint of experimental conditions for shortening the experimental period and increasing parameter sensitivities of the measurement data. A series of examinations showed that the use of sorptive tracer is advantageous for both obtaining measurement data that drastically changes during the transient state and increasing parameter sensitivities. However, these also depend on the selected experimental conditions, such as the dimensions of the specimen and reservoir. The effects of the tracer property and the other experimental conditions can be represented by the dimensionless reservoir volume defined as the ratio of the reservoir volume over the adsorptive capacity of the specimen. Therefore it is important to evaluate the value of the dimensionless reservoir volume, based on the available information for the testing material and the tracer, when designing experiments.

When the effective diffusion coefficient of the testing material is very small, the experimental duration for establishment of the equilibrium state becomes very long. A practical way of parameter estimation in such a case is inverse analysis of the transient data. In inverse analysis, a well-conditioned weighted Jacobian matrix is indispensable for accurately determining the values of the parameters of interest. A series of theoretical and numerical examinations revealed that the weighted Jacobian matrix for the proposed test is not necessarily well-conditioned, owing to differences between the orders of magnitude for the values of the effective diffusion coefficient and the capacity factor. The component values for the capacity factor, $\alpha$, in the weighted Jacobian matrix tend to be significantly lower than those for the effective diffusion coefficient, $D_e$. Thus, when compared to the $D_e$ value, computation of the $\alpha$ value tends to be more susceptible to roundoff errors, due to the singularity of the weighted Jacobian matrix. When the roundoff error is significant, the parameter estimation might be improved by working with the weighted Jacobian matrix defined by $\log(D_e)$ or both $\log(D_e)$ and $\log(\alpha)$ as alternative parameters. If the condition number is successfully lowered, the error in the parameter values will not be much larger than the error in the measurement.

In this study, ways of shortening the experimental duration and gaining parameter sensitivities were shown. However, several problems related to the inverse analysis have not been examined for the proposed test method. These should still be examined to clarify the feasibility of the proposed test. The problems are as follows. The uniqueness of the estimation results has not been guaranteed. In the gradient-based minimization algorithms, the parameters are iteratively searched along with the surface of the objective function on the parameter search domain; thus the shape of the objective function directly affects the uniqueness of the inverse analysis result. From the viewpoint of modeling, discrepancies between the test procedures and the analytical model introduce systematic errors into the measurement data, which directly affects the reliability of the estimation results. Specifically, sampling the solution from the reservoir for concentration measurements reduces the reservoir volume assumed to be constant in the analytical model. The systematic error caused by sampling might introduce significant errors in the parameter estimations. In addition, the uncertainty of the parameter estimation related to measurement error has not been examined. These problems related to the proposed diffusion test are currently being examined.

## REFERENCES

1. Neretnieks, I. (1980). Diffusion in the Rock Matrix: An Important Factor in Radionuclide Retardation? *Journal of Geophysical Research* 85(B8): 4379-4397.
2. Wadden, M. M., Katsube, T. J. (1982). Radionuclide Diffusion Rates in Igneous Crystalline Rocks. *Chemical Geology* 36: 191-214.

3. Lever, D. A., Bradbury, M. H., Hemingway, S. J. (1983). Modelling the Effect of Diffusion into the Rock Matrix on Radionuclide Migration. *Progress in Nuclear Energy* 12: 85-117.
4. Van Loon, L. R., Eikenberg, J. (2005). A High-Resolution Abrasive Method for Determining Diffusion Profiles of Sorbing Radionuclides in Dense Argillaceous Rocks. *Applied Radiation and Isotopes* 63: 11-21.
5. Muurinen, A. (1990). Diffusion of Uranium in Compacted Sodium Bentonite. *Engineering Geology* 28: 359-367.
6. Kim, H. T., Suk, T. W., Park, S. H. (1993). Diffusion for Ions through Compacted Na-Bentonite with Varying Dry Bulk Density. *Waste Management* 13: 303-308.
7. Cho, W. J., Oscarson, D. W., Hahn, P. S. (1993). The Measurement of Apparent Diffusion Coefficients in Compacted Clays: An Assessment of Methods. *Applied Clay Science* 8: 283-294.
8. Eriksen, T. E., Jansson, M., Molera, M. (1999). Sorption Effects on Cation Diffusion in Compacted Bentonite. *Engineering Geology* 54: 231-236.
9. Kozaki, T., Sato, Y., Nakajima, M., Kato, H., Sato, S., and Ohashi, H. (1999). Effect of Particle Size on the Diffusion Behavior of Some Radionuclides in Compacted Bentonite. *Journal of Nuclear Materials* 270: 265-272.
10. Sato, H., Suzuki, S. (2003). Fundamental Study on the Effect of An Orientation of Clay Particles on Diffusion Pathway in Compacted Bentonite. *Applied Clay Science* 23: 51-60.
11. Van Loon, L. R., Soler, J. M., Muller, W., Bradbury, M. H. (2004). Anisotropic Diffusion in Layered Argillaceous Rocks: A Case Study with Opalinus Clay. *Environmental Science & Technology* 38: 5721-5728.
12. Shackelford, C. D. (1991). Laboratory Diffusion Testing for Waste Disposal – A Review. *Journal of Contaminant Hydrology* 7: 177-217.
13. Lever, D. A. (1986). Some Notes on Experiments Measuring Diffusion of Sorbed Nuclides through Porous Media. Harwell Report, AERE R12321, 24 p.
14. García-Gutiérrez, M., Cormenzana, J. L., Missana, T., Mingarro, M., Molinero, J. (2006). Overview of Laboratory Methods Employed for Obtaining Diffusion Coefficients in FEBEX Compacted Bentonite. *Journal of Iberian Geology* 32: 37-53.
15. Van Loon, L. R., Jakob, A. (2005). Evidence for a Second Transport Porosity for the Diffusion of Tritiated Water (HTO) in a Sedimentary Rock (Opalinus clay-OPA): Application of Through- and Out-diffusion Techniques. *Transport in Porous Media* 61: 193-214.
16. Novakowski, K. S., van der Kamp, G. (1996). The Radial Diffusion Method .2. A Semianalytical Model for the Determination of Effective Diffusion Coefficients, Porosity, Arid Adsorption. *Water Resources Research* 32: 1823-1830.
17. Van Loon, L. R., Baeyens, B., Bradbury, M. H. (2005). Diffusion and Retention of Sodium and Strontium in Opalinus Clay: Comparison of Sorption Data from Diffusion and Batch Sorption Measurements, and Geochemical Calculations. *Applied Geochemistry* 20: 2351-2363.
18. Finsterle, S., Najita, J. (1998). Robust Estimation of Hydrogeologic Model Parameters. *Water Resources Research* 34: 2939-2947.
19. Carrera, J., Alcolea, A., Medina, A., Hidalgo, J., Slooten, L. J. (2005). Inverse Problem in Hydrogeology. *Hydrogeology Journal* 13: 206-222.
20. Carrera, J., Neuman, S. P. (1986). Estimation of Aquifer Parameters under Transient and Steady-State Conditions .1. Maximum-Likelihood Method Incorporating Prior Information. *Water Resources Research* 22: 199-210.
21. Finsterle, S., Persoff, P. (1997). Determining Permeability of Tight Rock Samples Using Inverse Modeling. *Water Resources Research* 33: 1803-1811.
22. Helmke, M. F., Simpkins, W. W., Horton, R. (2004). Experimental Determination of Effective Diffusion Parameters in the Matrix of Fractured Till. *Vadose Zone Journal* 3: 1050-1056.
23. Hollenbeck, K. J., Jensen, K. H. (1998). Maximum-Likelihood Estimation of Unsaturated Hydraulic Parameters. *Journal of Hydrology* 210: 192-205.

24. Finsterle, S., Faybishenko, B. (1999). Inverse Modeling of a Radial Multistep Outflow Experiment for Determining Unsaturated Hydraulic Properties. *Advances in Water Resources* 22: 431-444.
25. Romano, N., Santini, A. (1999). Determining Soil Hydraulic Functions from Evaporation Experiments by a Parameter Estimation Approach: Experimental Verifications and Numerical Studies. *Water Resources Research* 35: 3343-3359.
26. Kabala, Z. J. (2001). Sensitivity Analysis of a Pumping Test on a Well with Wellbore Storage and Skin. *Advances in Water Resources* 24: 483-504.
27. Knopman, D. S., Voss, C. I. (1987). Behavior of Sensitivities in the One-Dimensional Advection-Dispersion Equation: Implications for Parameter Estimation and Sampling Design. *Water Resources Research* 23: 253-272.
28. McElwee, C. D. (1987). Sensitivity Analysis of Groundwater Models. In: *Advances in transport phenomena in porous media*, Bear, J., Corapcioglu, M. Y., editors. NATO Advanced Study Institute Ser. E. 128: 751–817.
29. Wang, H. F., Hart, D. J. (1993). Experimental Error for Permeability and Specific Storage from Pulse Decay Measurements. *International Journal of Rock Mechanics and Mining Sciences & Geomechanics Abstracts* 30: 1173-1176.
30. McElwee, C. D., Bohling, G. C., Butler, J. J. (1995). Sensitivity Analysis of Slug Tests.1. The Slugged Well. *Journal of Hydrology* 164: 53-67